Use of MRI to identify enlarged inferior gluteal and ischioanal lymph nodes and associated findings related to the primary disease

Çağlar Uzun
Ayşe Erden
Ebru Düşünceli Atman
Evren Üstüner

PURPOSE
We aimed to draw attention to the lymph nodes at the inferior gluteal and ischioanal regions and evaluate the lesions accompanying them using 3.0 T magnetic resonance imaging (MRI).

METHODS
In total, 22 patients (15 men, 7 women; mean age, 50±11.2 years; age range, 32–71 years) were included in this study. The patients' medical records were reviewed. MRI data were reviewed on a picture archiving and communication system workstation by two radiologists in consensus. Lymph node location, laterality, number, and size were documented.

RESULTS
The primary disorders causing the enlargement of inferior gluteal lymph nodes (n=16) were perianal fistula of cryptoglandular origin (n=5), perianal fistula associated with Crohn's disease (n=2), decubitus ulcers (n=2), presacral abscess (n=1), non-Hodgkin lymphoma (n=2), prostate cancer invading urethra and anorectal junction (n=1), endometrium cancer invading the urethra and vagina (n=1), and anal cancer (n=2). The pathologies causing the enlargement of ischioanal lymph nodes (n=6) were perianal fistula of cryptoglandular origin (n=4), subcutaneous inflammation of gluteal region related to Crohn's disease (n=1), and prostate cancer (n=1).

CONCLUSION
The infectious and neoplastic lesions involving the anal canal, distal rectum, gluteal region, prostate, and urethra are the possible causes of inferior gluteal and ischioanal lymph node enlargement. Lymphoproliferative diseases can also affect these node groups. MRI is an important method to identify enlarged inferior gluteal and ischioanal lymph nodes and define associated findings.

From the Department of Radiology (Ç.U. ✉ cuzun77@ yahoo.com), Ankara University School of Medicine, Ankara, Turkey.

Magnetic resonance imaging (MRI) allows the assessment of nodal areas, which are inaccessible by routine surgical methods. The recognition of lymph node enlargement by MRI depends upon an increase in its size. Normal lymph nodes in gluteal and ischioanal regions are too small to be identified by imaging methods. MRI generally has the best soft tissue contrast among current techniques. High contrast of the lymph nodes against the surrounding suppressed fat on fat saturation MRI techniques (i.e., on turbo inversion recovery magnitude sequence), diffusion-weighted imaging (DWI) with high b value, and contrast-enhanced fat suppressed T1-weighted turbo spin-echo (TSE) imaging allows their detection.

The pattern of lymph node involvement depends principally on the site of the primary lesion and the natural pathways of local lymphatic drainage. Pelvic tumors drain to regional lymph nodes, the extent of which is described by the N stage in the TNM system, while metastases outside of the regional nodes are considered distant metastasis (M stage). This usually results in upstaging of the disease to overall stage IV cancer and may potentially affect the patient's prognosis and clinical management (1). Gluteal lymph nodes are the parietal group of the internal iliac nodes. They are subdivided into two parts as superior and inferior gluteal lymph nodes and located along the vessels of the same name. Lymph from the deeper (gluteal subfascial and visceral) tissues of the pelvis drains into these lymph nodes and then, into the internal and common iliac nodes before entering the lateral caval lumbar nodes. Ischioanal lymph nodes are located lateral to the anal canal. Lymph from the perineal tissues and anal canal can drain into these nodes (2–6).

Table 1. Imaging parameters for 3.0 T MRI

Parameter	T2W TSE	T2W TSE	T2W TSE (HR)	T2W TSE (HR)	DWI EPI b=50, 400,1000 s/mm²	TIRM*	T1W FS CE TSE
Matrix size	384×307	320×256	320×256	320×256	128×102	200×256	320×256
Slice thickness (mm)	3.5	5.0	3.0	3.0	5.0	5.0	3.5
Distance factor (%)	15	20	16	16	20	30	14
Repetition time (ms)	4500	5450	5460	5180	6445	4430	495
Echo time (ms)	104	93	58	58	70	35	12
Echo trains per slice	13	8	12	15	EPI factor: 180	10	39
Flip angle (degrees)	120	150	145	135	-	150	140
Reduction factor	2	2	2	2	2	2	2
NSA	2	3	4	4	5	2	3 (2 for oblique coronal)
FoV (mm)	220×220	220×220	180×180	180×180	360×280	200×200	200×200
Orientation	Sagittal	Axial	Oblique axial	Oblique coronal	Axial	Axial	Oblique axial/ oblique coronal
Bandwidth (Hz/Px)	250	260	260	260	2442	260	260
Acquisiton time (min:s)	4:05	2:18	4:54	6:00	5:09	3:08	4.31 (3:35 for oblique coronal)

T2W, T2-weighted; TSE, turbo spin-echo; HR, high resolution; DWI, diffusion-weighted imaging; EPI, echo planar imaging; TIRM, turbo inversion recovery magnitude; T1W, T1-weighted; FS, fat suppressed; CE, contrast-enhanced; NSA, number of signals acquired; FoV, field of view.
*Time of inversion (TI) is 140 ms.

The rate of lymph node involvement in inferior gluteal and ischioanal regions is unknown; however, according to our observations, the nodes in these locations rarely enlarge and are associated mostly with perineal lesions. To the best of our knowledge, until now, neither of these lymph node groups has been studied by imaging methods. The purpose of this study was to draw attention to the lymph nodes at the inferior gluteal and ischioanal regions and evaluate the lesions accompanying them by 3.0 T MRI.

Main points

- Infectious and neoplastic lesions involving the anal canal, distal rectum, gluteal region, prostate, or urethra and lymphoproliferative diseases are the possible causes of inferior gluteal and ischioanal lymph node enlargement.

- These nodes probably remain outside the target coverage of the irradiation beam and are inaccesible by routine surgical methods, therefore they can potentially influence clinical management and prognosis of the patients.

- MRI is an important method to identify enlarged inferior gluteal and ischioanal lymph nodes and define associated findings.

Methods

The institutional review board approved this retrospective study protocol and waived informed consent. Patients underwent MRI with a 3.0 T whole body system (MAGNETOM Verio, Siemens) using standard body matrixcoil. The imager operates with a maximum gradient strength of 45 mT/m and a slew rate of 200 T/m/s in all three directions. The pelvic MRI protocol consisted of standard sagittal and axial T2-weighted TSE images, axial DWI, high resolution (HR) oblique axial and oblique coronal turbo inversion recovery magnitude images, and HR oblique axial and oblique coronal contrast-enhanced fat suppressed T1-weighted TSE images. Oblique axial and coronal planes were orientated perpendicular and parallel to the anal canal, respectively. All pulse sequence parameters used in this study are listed in Table 1.

Radiology Information System/Picture Archiving and Communication System (RIS/PACS; Centricity 5.0 RIS-i, GE Healthcare) of our institution was utilized to identify patients with enlarged gluteal and ischioanal lymph nodes. The key words "inferior gluteal" and "ischioanal" were used for searching patients. The current study was intended to identify the gluteal and ischioanal lymph nodes and associated lesions and not to determine the prevalence of the condition. A total of 22 patients (15 men, 7 women; mean age, 50±11.2 years; age range, 32–71 years) with inferior gluteal or ischioanal lymph nodes were identified in our institution's RIS/PACS system during the interval between October 2011 and June 2015. The patients' medical records and clinical data retrieved from the hospital information system were reviewed.

MRI data retrieved from PACS were retrospectively evaluated by two radiologists in consensus. The properties of the lymph nodes and the probable causes that lead to enlargement were analyzed. Inferior gluteal lymph nodes were identified as well-defined, round, or oval structures of soft-tissue intensity at the fascial plane between the gluteus maximus muscle and obturator internus muscle, adjacent to the inferior gluteal vessels (Fig. 1a). Because the cross sections of the vessels were oval in shape at the axial plane, these nodes needed to be greater in diameter than the adjacent gluteal vessels to be recognized. By scrolling through the images, inferior gluteal vessels could be traced as tubular structures. The nodes ≥3 mm were perceptible and considerable, particularly when they were found

Table 2. Demographic data of patients, diagnoses, laterality, location, number, and size of lymph nodes

Patients	Age/sex	Diagnosis	LN laterality and location	LN number	LN size (mm)
1	34/M	Cryptoglandular perianal fistula	Left inferior gluteal	5	9/7/6/6/4
2	63/M	Cryptoglandular perianal fistula	Left inferior gluteal	3	8/3/3
3	43/M	Cryptoglandular perianal fistula	Left and right inferior gluteal	3	R: 5 L: 4/4
4	62/M	Cryptoglandular perianal fistula	Left inferior gluteal	3	3/3/3
5	32/M	Cryptoglandular perianal fistula	Right inferior gluteal	2	6/3
6	54/M	Perianal fistula related to CD	Right inferior gluteal	2	6/3
7	35/M	Perianal fistula related to CD	Left inferior gluteal	2	8/4
8	47/F	Gluteal decubitus ulcer	Right inferior gluteal	2	5/5
9	57/F	Gluteal decubitus ulcer	Right inferior gluteal	1	7
10	53/M	Healed perianal fistula associated with non-Hodgkin lymphoma	Right and left inferior gluteal	4	R: 4/3 L: 10/5
11	67/M	Invasive prostate cancer	Right inferior gluteal	3	20/18/15
12	60/M	Squamous cell anal cancer	Left inferior gluteal	1	7
13	66/M	Squamous cell anal cancer	Right inferior gluteal	3	11/8/4
14	50/M	non-Hodgkin lymphoma	Right inferior gluteal	2	5/5
15	71/F	Invasive endometrial cancer	Left inferior gluteal	2	9/5
16	48/F	Presacral abscess following TME for rectal cancer	Left inferior gluteal	5	4/3/3/3/3
17	47/F	Subcutaneous postcoccygeal/gluteal inflammation associated with CD	Right ischioanal	1	4
18	37/M	Cryptoglandular perianal fistula	Left ischioanal	1	4
19	39/F	Cryptoglandular perianal fistula	Right ischioanal	1	11
20	47/F	Cryptoglandular perianal fistula	Left ischioanal	1	11
21	48/M	Cryptoglandular perianal fistula	Right ischioanal	1	5
22	53/M	Prostate cancer	Left ischioanal	1	5

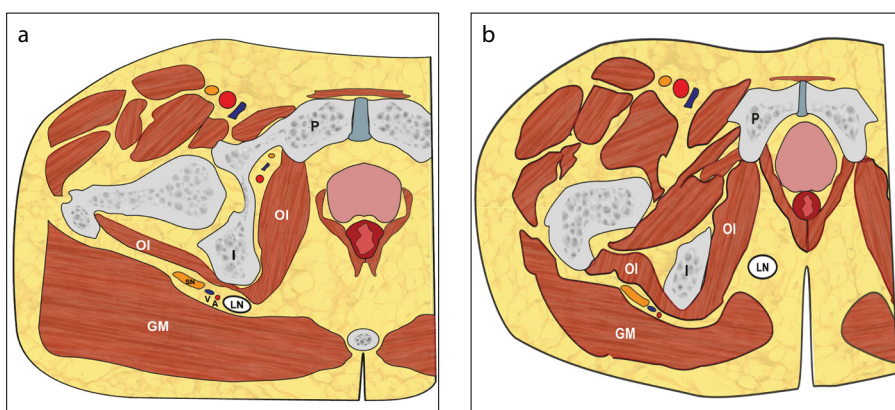LN, lymph node; M, male; R, right; CD, Crohn's disease; L, left; F, female; TME, total mesorectal excision.

Figure 1. a, b. Illustrations of inferior gluteal **(a)** and ischioanal **(b)** lymph node anatomy in the transverse plane. OI, obturator internus muscle; GM, gluteus maximus muscle; LN, lymph node; A, artery; V, vein; SN, sciatic nerve; I, ischium; P, pubic bone.

together with several larger nodes in the same location. Therefore, nodes having a size of ≥3 mm were considered as enlarged (Table 2). Ischioanal lymph nodes were identified as round or oval-shaped distinct structures within the fatty tissue of the ischioanal fossa, which is a paired triangular-shaped space lateral to the anal canal (Fig. 1b). For each patient, lymph node location, laterality, size, and number were recorded. Each short axis size (perpendicular to the longest diameter of the lymph node on the axial plane) was measured on the image using a caliper tool.

Results

The demographic data of the patients, diagnoses, location, laterality, number, and size of lymph nodes identified are presented in Table 2.

Enlarged lymph nodes were identified in the inferior gluteal region in 16 patients. There were a total of 43 lymph nodes in the inferior gluteal group. In two patients, the inferior gluteal nodes were bilaterally involved. The diameter of the inferior gluteal lymph nodes varied between 3 and 20 mm (mean, 6.04±3.89 mm) in the short axis.

Five of the 16 patients with inferior gluteal lymph node enlargement had transsphincteric perianal fistula of cryptoglandular origin (idiopathic; probably related

to anal gland infection) (Fig. 2) and two had perianal fistula associated with Crohn's disease. The nodes were limited only to this site in four patients who had perianal fistula of cryptoglandular origin.

Other causes of the inferior gluteal lymph node enlargement were gluteal decubitus ulcer (n=2); non-Hodgkin lymphoma (n=2); presacral abscess following total mesorectal excision (TME) for rectal cancer (n=1); pros-tate cancer invading urethra and anorectal junction (n=1) (Fig. 3); endometrium cancer invading the sigmoid colon, urinary bladder, urethra, and vagina (n=1); and squamous cell anal cancer (n=2). Four patients (patient no: 6, 10, 14, and 19 in Table 2) also had ip-silateral enlarged superior gluteal lymph nodes.

Enlarged lymph nodes were identified at the ischioanal fossa in six patients. No patient had lymph nodes at both inferior gluteal and ischioanal locations.

The primary pathologies causing the enlargement of ischioanal nodes were intersphincteric (n=3) (Fig. 4) and transsphincteric (n=1) perianal fistulas of criptoglandular origin, subcutaneous inflammation of the postcoccygeal and gluteal region in a patient with Crohn's disease (n=1), and prostate cancer (n=1). The diameter of the ischioanal nodes varied between 4 and 11 mm (mean, 6.66±3.38 mm) in the short axis.

Discussion

In this study, we aimed to draw attention to the inferior gluteal and ischioanal lymph nodes, which are affected in very rare instances. Only very limited information is available in the literature about the gluteal lymph nodes. To the best of our knowledge, until now, no study has been conducted on this subject; at least in the medical imaging area. There is only one case report that describes superior gluteal lymph node metastasis from a posterior loin melanoma (2).

As far as we are concerned, nodal involvement in cryptoglandular perianal fistula has not been addressed in the literature. We showed that the most common disease associated with inferior gluteal and ischioanal lymph node enlargement was perianal fistula. Fistula was present in half of the patients (11 out of 22 patients) with enlarged nodes
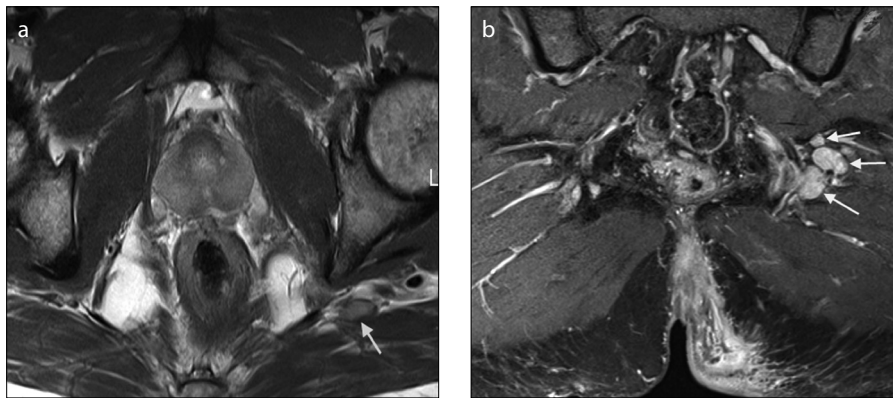

Figure 2. a, b. A 34-year-old man with left complex transsphincteric fistula. Axial T2-weighted turbo spin-echo (TSE) image through lower pelvis **(a)** shows left inferior gluteal lymph node *(arrow)*. Oblique coronal contrast-enhanced fat suppressed T1-weighted TSE image **(b)** shows three distinct inferior gluteal lymph nodes *(arrows)*. Note also contrast-enhanced inflammatory changes in the left gluteal subcutaneous fat tissue.
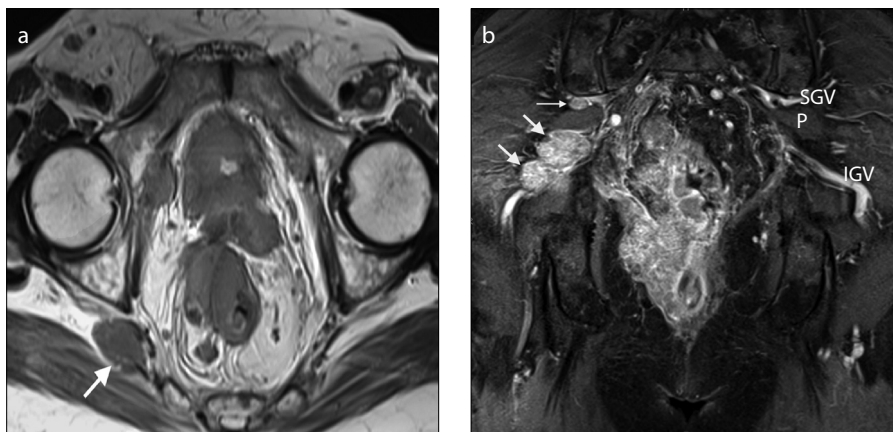

Figure 3. a, b. A 67-year-old man with locally advanced prostatic cancer infiltrating bladder base, seminal vesicles, deep perineal space, bilateral external obturator muscles, pubic bone, and rectum. Axial T2-weighted TSE image through lower pelvis **(a)** shows right inferior gluteal lymph node *(arrow)*. Oblique coronal contrast-enhanced fat suppressed T1-weighted TSE image **(b)** shows superior *(thin arrow)* and inferior *(thick arrows)* gluteal lymph nodes. SGV, superior gluteal vessels; P, piriformis muscle; IGV, inferior gluteal vessels.
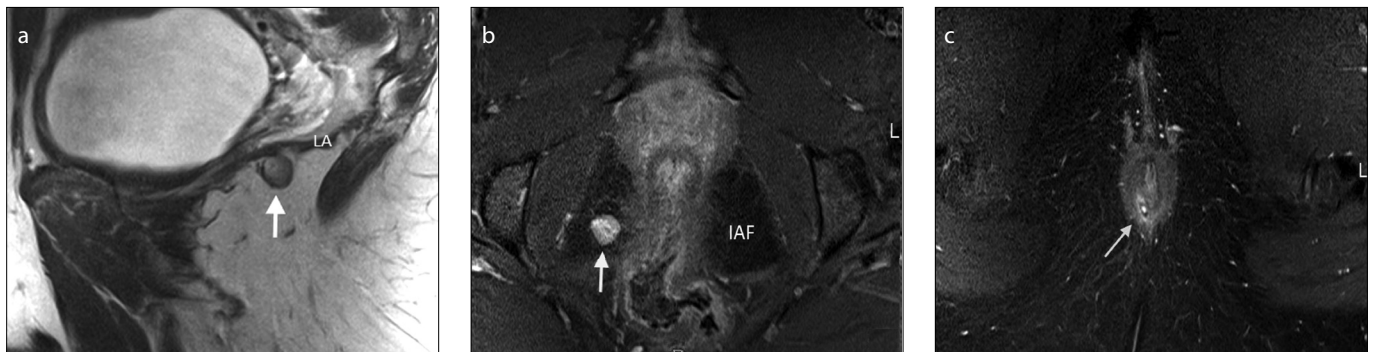

Figure 4. a–c. A 39-year-old woman with intersphincteric fistula. Right parasagittal T2-weighted TSE image **(a)** shows well-defined soft-tissue nodule, 11 mm in diameter in ischioanal fossa *(arrow)*. Oblique axial contrast-enhanced fat suppressed T1-weighted TSE images **(b, c)** show enlarged right ischioanal lymph node **(b,** *arrow)* and intersphincteric fistula posteriorly at 7 o'clock, contained by external anal sphincter **(c,** *arrow)*. There is no tract in ischioanal fossa. LA, iliococcygeal component of levator ani muscle; IAF, ischioanal fossa.

in these locations and was usually of idiopathic (cryptoglandular infectious) origin. Our patients with enlarged inferior gluteal lymph nodes had mostly transsphincteric type fistulas. These lymph nodes were also observed in Crohn's disease with complex perianal sepsis. Decubitus ulcer and lymphoproliferative disorders manifesting with perianal inflammation were the other diseases in patients with prominent nodes. We found that these nodes were enlarged in the presence of cancers of the distal anal canal; endometrium cancer invading the vagina, urethra, and urinary bladder; and prostate cancer invading the urethra and the anorectal region.

MRI is the imaging modality of choice to investigate the anal region in both in perianal fistula and anal cancer (7–10). This method has a major impact on the preoperative assessment of perianal fistulas to improve patient outcome (11). MRI has been recommended by the European Society for Medical Oncology (7) as the preferred modality of choice to stage anal cancer, taking into account the maximum tumor diameter, invasion of adjacent structures, and regional lymph node involvement. The incidence of regional nodal involvement increases with primary tumor size (12).

MRI is also helpful in determining the depth and extent of soft tissue involvement underlying decubitus ulcers and shows accompanying fluid collections, osteomyelitis, heterotopic bone formation, and adjacent bone marrow edema (13).

In a few patients, we also identified enlarged ischioanal lymph nodes. In total, three out of four patients with enlarged ischioanal nodes had intersphincteric fistula located in the distal half of the anal canal. The tracks ran between the internal and external sphincters close to the posterior midline (at 5–7 o'clock) and reached the perianal skin through or medial to the subcutaneous external sphincter. The ischioanal fossa, previously known as the ischiorectal fossa, is a fat-filled space of the perineum and contains lymphatic trunks, internal pudendal vessels and nerves, posterior scrotal (labral) vessels and nerves, and fibroelastic connective tissue fibers. Metastasis to ischioanal fossa is uncommon, although this region contains a rich blood supply and considerable amount of lymphatics. The possible causes of the metastatic lymphadenopathy in this space were anorectal and prostatic carcinoma (14). Although lymph from the anal canal below the dentate line usually drains to the inguinal nodes, it can also drain into the inferior rectal lymphatics and to the ischioanal fossa, if the primary drainage is obstructed (14). The nodes in the ischioanal fossa are at risk for harboring metastases from the cancers of the distal rectum, anal canal, Bartholin's glands, prostate, and urinary bladder. Lymphoma can also cause the lymph nodes to become enlarged in the ischioanal space (3–6, 15–18).

This study had some limitations such as having a relatively small sample size and the absence of histopathologic confirmation of nodal involvement. These limitations can affect the overall generalization of our findings but would not prevent us from making inferences about the origin of the lymphatics draining into these lymph nodes. There is a lack of studies on this topic to compare our results. As more effort is put into searching for lymph nodes in such atypical sites, the more will become evident. MRI is an important assessment tool for the evaluation of these nodes and associated lesions in the lower part of the pelvis and perineum.

In conclusion, gluteal and ischioanal regions are rare sites for nodal involvement of different pelvic disorders. Most of our patients, who had enlarged inferior gluteal and ischioanal lymph nodes on MRI, had an anal and/or gluteal inflammation or infection. This is consistent with the fact that such disorders are much more common than the neoplasms of this region. Distal rectal, perineal, prostatic, and urethral diseases are the other associated disorders. In malignant processes, these groups of lymph nodes are at risk for harboring metastases if the primary disease is extensive or advanced. In addition, one should note that these nodes probably remain outside of the target coverage of the irradiation beam and are inaccessible by routine surgical methods; therefore, they can potentially influence the clinical management and prognosis of the patients.

Conflict of interest disclosure
The authors declared no conflicts of interest.

References

1. McMahon CJ, Rofsky NM, Pedrosa I. Lymphatic metastases from pelvic tumors: anatomic classification, characterization, and staging. Radiology 2010; 254:31–46. [CrossRef]

2. Fujiwara M, Nagata T, Matsushita Y, et al. Superior gluteal lymph node metastasis of melanoma. J Dermatol 2013; 40:852–853. [CrossRef]

3. O'Rahilly R, Müller F, Carpenter S, et al. Blood vessels, nerves and lymphatic drainage of the pelvis. In: Basic human anatomy. A regional study of human structure [Dartmouth Medical School Web site], 2008. Available at: http://www.dartmouth.edu/humananatomy/part_6/chapter_32.html. Accessed January 15, 2015.

4. Richter E, Feyerabend T. Normal lymph node topography CT atlas. Berlin: Springer-Verlag, 2004; 113–147. [CrossRef]

5. Lentz GM, Lobo RA, Gershenson DM. Comprehensive gynecology. 6th ed. Philadelphia: Elsevier Mosby, 2012; 54.

6. Stranding S. Grays Anatomy: The anatomical basis of clinical practice. 40th ed. Spain: Churchill Livingstone, 2008; 1349–1387.

7. Glynne-Jones R, Northover JM, Cervantes A. ESMO Guidelines Working Group. Anal cancer: ESMO clinical practice guidelines for diagnosis, treatment and follow-up. Ann Oncol 2010; 21:87–92. [CrossRef]

8. de Miguel Criado J, del Salto LG, Rivas PF, et al. MR imaging evaluation of perianal fistulas: spectrum of imaging features. Radiographics 2012; 32:175–194. [CrossRef]

9. Halligan S, Stoker J. Imaging of fistula in ano. Radiology 2006; 239:18–33. [CrossRef]

10. George U, Sahota A, Rathore S. MRI in evaluation of perianal fistula. J Med Imaging Radiat Oncol 2011; 55:391–400. [CrossRef]

11. Parks AG. Pathogenesis and treatment of fistula-in-ano. Br Med J 1961; 5224:463–469. [CrossRef]

12. Tonolini M, Bianco R. MRI and CT of anal carcinoma: a pictorial review. Insights Imaging 2013; 4:53–62. [CrossRef]

13. Hencey JY, Vermess M, van Geertruyden HH, et al. Magnetic resonance imaging examinations of gluteal decubitus ulcers in spinal cord injury patients. J Spinal Cord Med 1996; 19:5–8.

14. Llauger J, Palmer J, Pérez C, et al. The normal and pathologic ischiorectal fossa at CT and MR imaging. Radiographics 1998; 18:61–82. [CrossRef]

15. Guo XF, Wang L, Yang ZL, et al. Lymph nodes distribution and metastatic pattern of ultra-low rectal cancer after neoadjuvant therapy. Zhonghua Wei Chang Wai Ke Za Zhi 2012; 15:1053–1056.

16. Anaf V, Buxant F, Rodesch F, et al. Adenoid cystic carcinoma of Bartholin's gland: what is the optimal approach? Eur J Surg Oncol 1999; 25:406–409. [CrossRef]

17. Dundr P, Pesl M, Povýsil C, et al. Large cell neuroendocrine carcinoma of the urinary bladder with lymphoepithelioma-like features. Pathol Res Pract 2003; 199:559–563. [CrossRef]

18. Tappouni RF, Sarwani NI, Tice JG, et al. Imaging of unusual perineal masses. AJR Am J Roentgenol 2011; 196:412–420. [CrossRef]